Structure of Oriented Polystyrene Monofilaments and Its Relationship to Brittle-to-Ductile Transition

YOSHIKAZU TANABE and HISAAKI KANETSUNA, *Research Institute for Polymers and Textiles, Kanagawa-ku, Yokohama 221, Japan*

Synopsis

Oriented atactic polystyrene monofilaments show brittle-to-ductile transition in the vicinity of a degree of birefringence $\Delta n = -2 \times 10^{-3}$ (at a temperature of 20°C and at the stretching rate of 100%/min) independently of the various spinning conditions. The amorphous orientation of a cylindrically symmetric system was investigated by wide-angle x-ray scattering experiments. The orientation of polystyrene monofilaments in real space is denoted by $P_2(\cos \alpha)$ within the precision of measurement. The coefficient $D_2(r)$ of the second term in an expansion of cylindrical distribution function in spherical harmonics has two main peaks, near $r = 1.6$ Å and $r = 4 \sim 5$ Å. The negative peak near $r = 1.6$ Å indicates orientation of phenyl groups in a plane perpendicular to the fiber axis. The positive peak near $r = 5$ Å (brittle region) or near $r = 4$ Å (ductile region) indicates the piling up of phenyl groups for the direction of the fiber axis. It is most probable that the amorphous state of atactic polystyrene consists of an appropriate cohesion of planar zigzag chains of syndiotactic polystyrene. The lower spacing ($r = 4$ Å) of the positive second peak in ductile region suggests that there are interchain phenyl groups near $r = 5 \sim 6$ Å in a plane perpendicular to the fiber axis and that the molecular chains are extended parallel to the direction of the fiber axis. This parallel packing of chain segments along the fiber axis suppresses the formation and growth of cracks of polystyrene monofilaments resulting in ductile fracture.

INTRODUCTION

In a previous study[1] atactic polystyrene monofilaments having various degrees of orientation were obtained by the spinning method where molten polystyrene is extruded directly into a bath (ethanol and water) or surrounding air maintained below the glass transition temperature (−70° to +50°C). The degree of orientation can be changed mainly by the winding velocity. The brittle-to-ductile transition in these polystyrene monofilaments has been found in relation to the draft dependence of their elongation at break, where draft is defined by the ratio of linear output velocity at the nozzle to the winding velocity. And by using the degree of birefringence Δn as a parameter of amorphous orientation, the elongation at break can be represented by a curve independently of various spinning conditions such as distance between nozzle and guiding roll directly under the nozzle, nozzle temperature, and the temperature of the cooling bath (−70° to +50°C). Its brittle-to-ductile transition takes place at ca. $\Delta n = -2 \times 10^{-3}$ at a temperature of 20°C and at a stretching rate of 100%/min. Other mechanical properties such as tensile strength, Young's modulus, yield stress, and yield strain can be represented by a curve, and the transition point appears at ca. $\Delta n = -2 \times 10^{-3}$ similarly.

The tensile strength (nominal) of polystyrene monofilaments increases monotonically with increasing Δn in the ranges of $|\Delta n| < |-2 \times 10^{-3}|$ and $|\Delta n| > |-2 \times 10^{-3}|$; and in the vicinity of $\Delta n = -2 \times 10^{-3}$, a transition point is faintly recognized (Fig. 2). But true tensile strength (corrected for filament area) would

Journal of Applied Polymer Sciences, Vol. 22, 1619–1630 (1978)

0021-8995/78/0022-1619$01.00

show a distinct discontinuous transition point in the vicinity of $\Delta n = -2 \times 10^{-3}$ since cross sections of these monofilaments drastically decrease at this transition point with increase in elongation at break. Young's modulus increases monotonically as $|\Delta n|$ increases. Since the yield points have not been observed in the range of $|\Delta n \lesssim |-2 \times 10^{-3}|$, yield stress and yield strain are significant in the range of $|\Delta n| \gtrsim |-2 \times 10^{-3}|$. Yield stress increases monotonically as $|\Delta n|$ increases in the range of $|\Delta n| \gtrsim |-2 \times 10^{-3}|$. Yield strain is constant or decreases rather slightly as $|\Delta n|$ increases from ca. $|-2 \times 10^{-3}|$.

When tensile strength in the brittle region and yield stress in the ductile region are plotted simultaneously for Δn, these curves intersect each other at the transition point $\Delta n = -2 \times 10^{-3}$. The same occurs in the case of elongation at break in the brittle region and yield strain in the ductile region.

Mechanical properties show brittle-to-ductile transition in their draft dependence. But the degree of birefringence does not show a transition in its draft dependence. This fact suggests that this brittle-to-ductile transition of amorphous atactic polystyrene is related to more microscopic structure than the range of light wavelengths.

In this study the amorphous orientation of atactic polystyrene was investigated by wide-angle x-ray scattering experiments and the relation of elongation at break with the microscopic structure of the amorphous state is discussed.

The cylindrical distribution function $D(r,\alpha)$ can be expanded to[3-6]

$$D(r,\alpha) = \sum_{n=0}^{\infty} D_{2n}(r)\, P_{2n}(\cos \alpha) \tag{1}$$

where r and α are the spherical coordinates of a point in real space, as shown in Figure 1, and P_{2n} is the Legendre polynomial of order $2n$. From the uniaxial symmetry in relation to the fiber axis, only terms of order $2n$ are retained. The scattering intensity has a similar symmetry, and expansion in spherical harmonics leads to the expression

$$I(S,\varphi) = \sum_{n=0}^{\infty} I_{2n}(S)\, P_{2n}(\cos \varphi) \tag{2}$$

where S and φ are the spherical coordinates in reciprocal space, $S = (2/\lambda) \sin \theta$, 2θ is the scattering angle, λ is the wavelength of x-rays, and

$$I_{2n}(S) = \frac{4n+1}{2} \int_0^{\pi} I(S,\varphi)\, P_{2n}(\cos \varphi) \sin \varphi \, d\varphi \tag{3}$$

$$D_{2n}(r) = (-1)^n 4\pi \int_0^{\infty} S^2 I_{2n}(S)\, j_{2n}(2\pi S r)\, dS \tag{4}$$

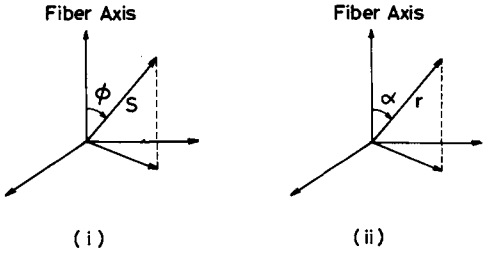

Fig. 1. Coordinate systems in (i) reciprocal and (ii) real space for a cylindrically symmetric system.

where j_{2n} is the spherical Bessel function of order $2n$. The difference intensity from the isotropic patterns, $I'(S,\varphi)$, includes all the information of orientation in the amorphous state and using this difference intensity,

$$I_{2n}(S) = \frac{4n+1}{2} \int_0^\pi I'(S,\varphi) P_{2n}(\cos\varphi) \sin\varphi \, d\varphi \tag{5}$$

is obtained from eq. (3). In experiment, eq. (5) is very convenient because various corrections such as incoherent scattering and air scattering are not necessary to obtain $I_{2n}(S)$ and $D_{2n}(r)$.

By analyzing coefficients $D_{2n}(r)$, the amorphous structure of polystyrene monofilaments is investigated. Its relation to brittle-to-ductile transition is discussed.

EXPERIMENTAL

Commercial polystyrene (Styron 679, $\overline{M}_w = 1.84 \times 10^5$, $\overline{M}_w/\overline{M}_n = 2.8$) was spun by a screw-type extruder under the following conditions: molten polymer temperature 197°C, diameter of each nozzle hole 0.5 mm (a nozzle having five holes was used), distance between nozzle and guiding roll directly under the nozzle 81 cm, output rate 5 g/min, and temperature of surrounding air 12°C. Average diameter and degree of birefringence measured by using daylight (wavelength 550 mμ) of each sample are shown in Table I. Draft dependence of Δn is shown in Figure 8.

Tensile strength (nominal) and elongation at break (nominal) are shown in Figure 2 for these samples measured under room temperature of 20°C, stretching rate 20 mm/min, and distance between jaws 20 mm. In measuring the wide-angle x-ray scattering intensities, a diffractometer (Geigerflex 2027, Rigaku Electric Co., Ltd.) was used with Ni-filtered CuK_α radiation, a pulse height analyzer, and a scintillation counter. The diameter of the pinhole was set at 2 mm, and the angle of the receiving slit was ca. 0.65°. The symmetric transmission method was used. Monofilaments of polystyrene were arranged side by side in parallel and put in layers so as to become about 0.8 mm thick.

Intensity measurements were made by scanning the range of 4.4°–40° of scattering angle 2θ at each value of χ, which is equal to $90° - \varphi$. And χ was changed from 0° to 90° at intervals of 9°. Scattered intensities were added up for 10 sec in order to obtain 10^3–10^4 counts over the scattering angle measured. Polarization and absorption factors were corrected. The absorption factor was approximately corrected by using the correction equation for plate. Calculation was carried out with the aid of a HITAC 8450 digital computer.

TABLE I
Diameters and Degree of Birefringence of Specimens Used in Wide-Angle X-Ray Scattering Experiments

	Sample no.						
	15	17	14	13	12	11	16
Diameter, μ	259	205	190	154	104	72.8	61.0
Degree of birefringence × 10^{-3}	−0.72	−1.24	−1.61	−2.35	−5.23	−9.56	−12.8

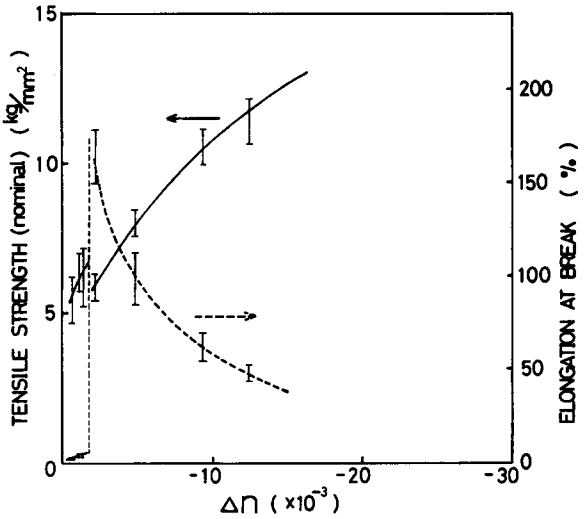

Fig. 2. Dependence of degree of birefringence (Δn) on tensile strength (nominal) and elongation at break (nominal) for atactic polystyrene monofilaments.

RESULTS AND DISCUSSION

Amorphous Orientation

The deviation of scattering intensity from the isotropic one is expressed by $I_{2n}(S)$. Coefficients $I_2(S)$ are plotted in Figure 3. The other coefficients such as $I_4(S)$ and $I_6(S)$ do not depend on S and are equal to zero within the precision of measurement. This result shows that the orientational behavior of atactic polystyrene in reciprocal space can be described by eq. (6) with sufficient precision:

$$P_2(\cos\varphi) = \frac{3\cos^2\varphi - 1}{2} \tag{6}$$

It is clear that there is a positive peak in the vicinity of $S = 0.23$ for all specimens, and this peak increases monotonically as draft or degree of birefringence Δn increases. A negative peak in the vicinity of $S = 0.11$ specimens 12, 11, and 16 for which the degree of birefringence is larger.

Deviations of distribution function from isotropic (radial distribution function), $D_{2n}(r)$, were calculated from eq. (4). Corresponding to the fact that $I_4(S)$, $I_6(S)$, etc., are almost equal to zero except $I_2(S)$, deviations such as $D_4(r)$ and $D_6(r)$ are almost equal to zero. $D_2(r)$ for each specimen is plotted in Figure 4. These oriented atactic polystyrene monofilaments have the following orientational characteristics:

$$P_2(\cos\alpha) = \frac{3\cos^2\alpha - 1}{2} \tag{7}$$

in real space, which are similar to those in reciprocal space. It should be noted that in transforming to $D_2(r)$ according to eq. (4), ripples due to truncation errors arise with the period of $r = 3.3$ Å. But in our results, ripples are hardly ever observed.

In Figure 4, there is a negative peak in the vicinity of $r = 1.6$ Å for all specimens.

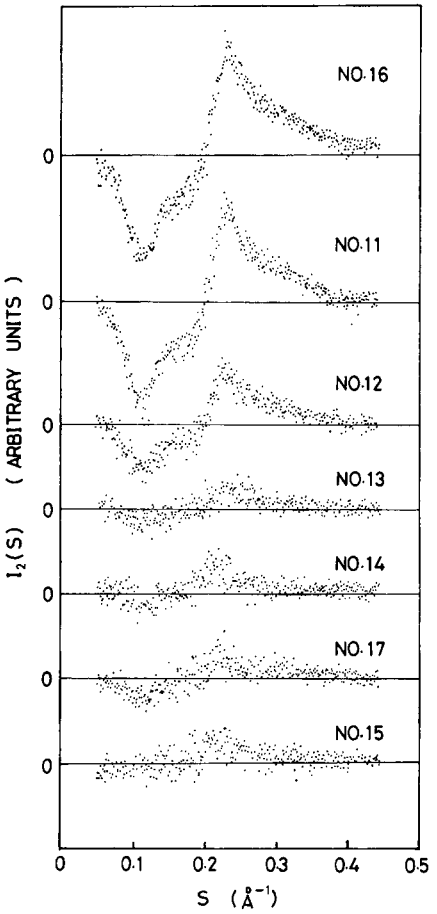

Fig. 3. Coefficient of deviation from isotropic intensity patterns $I_2(S)$ vs S for various oriented atactic polystyrenes.

The height of this peak increases with increase in draft or degree of birefringence Δn. For specimens 13, 12, 11, and 16, there is a positive peak in the vicinity of $r = 4$ Å, and this peak height decreases monotonically and more sharply near $r = 5$–6 Å with increasing r. For specimens 14, 17, and 15, there is a positive peak near $r = 5$ Å. This fact suggests that the drastic increase in elongation at break (Fig. 2) has some relation to the absence of the peak near $r = 5$ Å or to a shift to lower spacings (near $r = 4$ Å). This problem is discussed later.

For an interpretation of $D_2(r)$, it should be first considered that the coherent scattering between phenyl groups in a chain or two chains is of importance because the number of carbon atoms in a phenyl group is three times as large as in the main chain per monomer. Significant peaks in $D_2(r)$ are in the vicinity of $r = 1.6$ Å and $r = 4$–5 Å. As shown by Wecker et al.,[7] intramolecular scattering contributes to the peak in the vicinity of $r = 1.6$ Å, and both intra- and intermolecular scattering contribute to the peak in the vicinity of $r = 4$–5 Å. The signs of these two peaks show that the peak near $r = 1.6$ Å represents the C—C vector perpendicular to the fiber axis and the one near 4–5 Å represents the C—C vector parallel to it. A planar zigzag chain model for syndiotactic polystyrene is very suitable for the model satisfying the above conditions. Phenyl groups in a planar

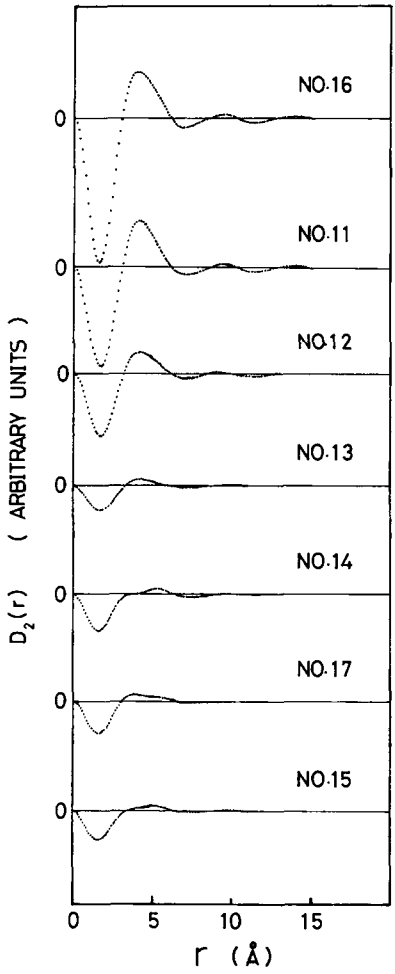

Fig. 4. Coefficient of deviation from radical distribution function $D_2(r)$ vs r for various oriented atactic polystyrenes.

zigzag chain of syndiotactic polystyrene are set perpendicular to the chain axis. The distances between the carbon atoms of this model are shown in Figure 5. The oriented amorphous state of atactic polystyrene consists mainly of these planar zigzag chains the chain axes of which are oriented to the fiber axis with distribution of $P_2(\cos \alpha)$. In this model the phenyl groups are inclined per-

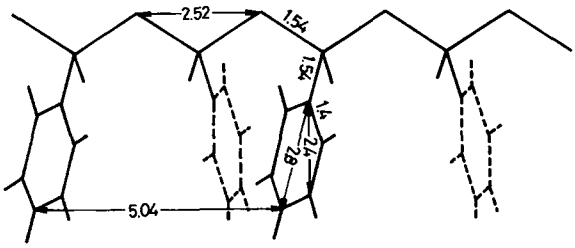

Fig. 5. Distances between carbon atoms in planar zigzag conformation of syndiotactic polystyrene, in units of Å.

pendicular to the fiber axis, and it is not in conflict with the fact that the degree of orientation Δn is negative for these oriented polystyrene monofilaments (see Fig. 8).

In the above-mentioned model, the C—C distances in a phenyl group are 1.4, 2.4, and 2.8 Å, and these distances are included in the negative peak near $r = 1.6$ Å in $D_2(r)$. The distance between the second-nearest neighbor phenyl groups along the main chain direction is 5.04 Å, and this contributes to the positive peak near $r = 5$ Å in $D_2(r)$. Therefore, the experimental results for samples 14, 17, and 15 can be interpreted by this planar zigzag model qualitatively. But the spacings of the positive second peak for samples 13, 12, 11, and 16 are lower than the described one in our model.

It should be noted that the 5.04 Å distance is the most probable and the nearest one in the distances contributing to $D_2(r)$ from phenyl groups along the main chain. The reason is as follows: The first-nearest neighbor phenyl groups in an atactic polystyrene chain are possibly 2.5, 5.4, 6.4, and 7.3 Å apart. Conformational energy consideration reduces the existence probability at 2.5 Å. The others are not in the direction of the chain axes. The second- or higher-order nearest neighbor phenyl groups have various distances according to various conformations of the main chain, but the possibility that these vectors tend toward the fiber or main-chain axis is very small except special conformations such as zigzag conformation for a syndiotactic chain and 3_1 helix conformation for an isotactic chain. Accordingly, these intramolecular vectors contribute mainly to the isotropic intensity pattern and less to $D_2(r)$. For zigzag conformation of a syndiotactic chain, the second-nearest neighbor phenyl groups have a 5.04 Å distance along the fiber axis as mentioned above; and for 3_1 helix conformation of an isotactic chain, the third-nearest neighbor phenyl groups are along the fiber axis the distance of which is 6.65 Å. This distance is larger than the one for a zigzag chain.

The above considerations suggest that contribution to $D_2(r)$ from the intermolecular scattering is very important. If there are C—C vectors between two chains, which are perpendicular to the fiber axis and are 5–6 Å long, these influences appear negative in $D_2(r)$. Contribution to $D_2(r)$ from intramolecular distances ~5 Å is positive and that from intermolecular distances 5–6 Å is negative, and the summation of these contributions results in the positive peak near 4 Å and a steeper downward slope at 5–6 Å for specimens of higher degree of orientation.

This conjecture is supported by the facts that the density of these specimens is ca. 1.043 g/cm^3 (see Fig. 9) and that these monofilaments have a uniaxial symmetry. Considering these facts, two models are considered for the packing model of planar zigzag chains of syndiotactic polystyrene, which are shown in Figure 6 (model 1) and Figure 7 (model 2). Model 1 has a rhombic cross-sectional unit cell in the x-y plane one side of which is 15.09 Å long, and model 2 has a unit cell of hexagonal cross section one side of which is 8.71 Å long. These side lengths were obtained on the basis that (i) the intramolecular distance of the first-nearest neighbor phenyl groups in the x-y plane is 4.80 Å and their intermolecular distance is at most the same; (ii) the distance between repeat units along the zigzag chain axis (z-axis) is 5.04 Å; and (iii) the density is about 1.043 g/cm^3. The phenyl groups represented by solid lines and those represented by dotted lines differ by 2.52 Å in height along the z-axis. These models are aimed at studying the

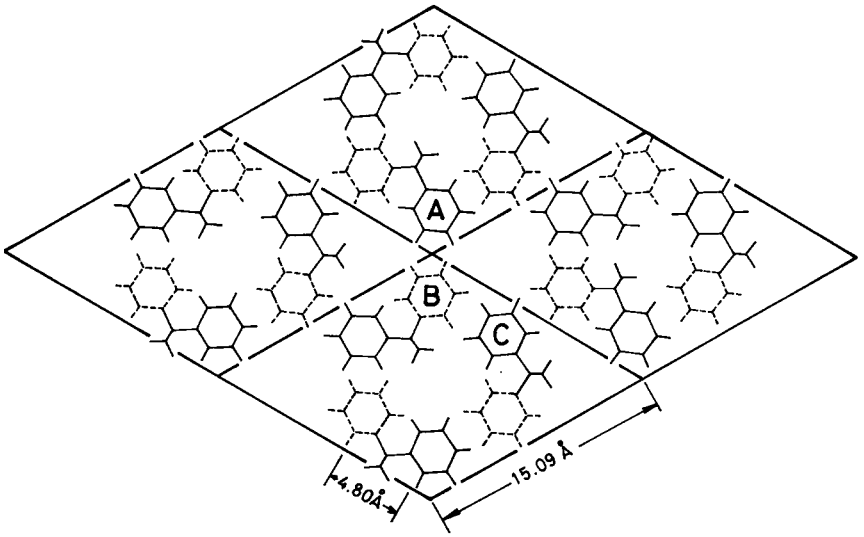

MODEL 1

Fig. 6. Model 1 for the packing of planar zigzag conformation of syndiotactic polystyrenes. Unit cell has a rhombic cross section with side 15.09 Å long. Density for this packing is ca. 1.042 g/cm^3.

packing of phenyl groups; the position of the main chain is not so significant since, as mentioned above, the coherent scattering between phenyl groups contributes mainly to the observed scattering intensity of polystyrene. Moreover, if a real amorphous state could be represented by these models, the main chains are rather more randomly packed than in models 1 and 2 by reason of distribution of intermolecular distances and z-coordinates (due to bending, kinking, etc.). The directions of unit cells are also not significant. It should be considered that only averaged positions are denoted in Figures 6 and 7 and that in these models distances between the first-nearest neighbor chains or the second are significant; positions of chains apart from the second-nearest neighbor chains or the third are of little significance since there would be various disorders in a real amorphous state.

In model 1, the nearest neighbor distance in the x-y plane between the intermolecular phenyl groups (A and B or B and C groups) is about 5 Å, but the height along the z-axis is different. These vectors in the amorphous state will contribute to the isotropic scattered intensity if various orientations of phenyl rings are considered. The second-nearest neighbor distance (A and C groups, etc.) is ca. 8.6 Å, and these vectors are in x-y plane. Influences of these vectors can appear negative in the vicinity of r = 8.6 Å in $D_2(r)$. The intramolecular vectors of 5.04 Å length and directed to the z-axis contribute positively to $D_2(r)$ at ca. 5 Å. Accordingly, $D_2(r)$ has a positive peak near 5 Å and a negative one near 8 Å.

In model 2, the two nearest neighbor phenyl groups (for example, B and C groups) have necessarily the same height along the z-axis in the three nearest neighbor groups (A, B, and C groups). This situation arises in the other three nearest neighbor groups in this model. The distance of these nearest neighbor phenyl groups having the same height is about 6 Å. These vectors contribute

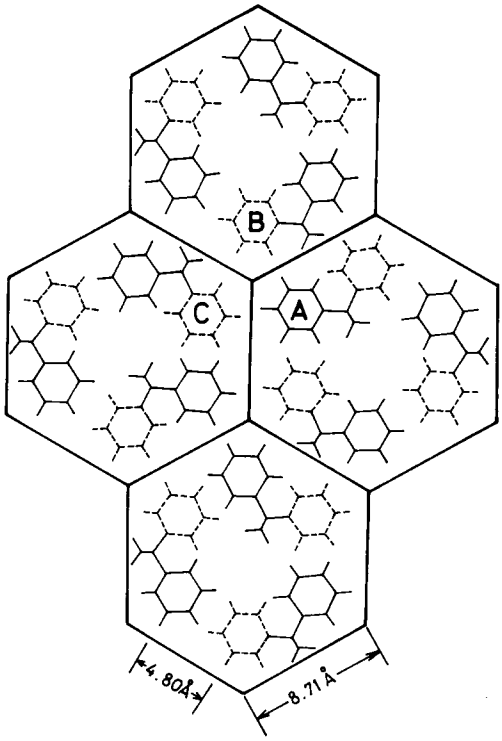

Fig. 7. Model 2 for the packing of planar zigzag conformation of syndiotactic polystyrenes. Unit cell has a hexagonal cross section with side 8.71 Å long. Density for this packing is ca. 1.043 g/cm^3.

negatively to $D_2(r)$ at ca. 6 Å. Intramolecular spacings between second-nearest neighbor phenyl groups contribute positively to $D_2(r)$ near 5 Å, similar to model 1. Therefore, $D_2(r)$ has a positive peak near 5 Å and a negative one near 6 Å. As the result of summation of these contributions of different signs, the steeper downward slope appears near 5–6 Å, and the position of the peak apparently shifts to lower spacings.

The real oriented amorphous structures of polystyrene monofilaments are perceived as follows by noticing the short-range order structure. The oriented amorphous structure in the brittle region (specimens 15, 17, and 14) seems to be almost the same as the isotropic amorphous state, except that there are syndiotactic chain segments stretched and oriented along the fiber axis here and there. These oriented segments are ca. 6 Å apart. If the oriented part is not a chain segment but a collection of chain segments, the structure seems to include various disorders along the x-, y-, and z-axes based on the lattice of model 1. In any case, the amorphous structure in this brittle region is nearly isotropic and main chains are scarcely oriented to the fiber direction. The oriented amorphous structure in the ductile region (specimens 13, 12, 11, and 16) seems to be the structure that includes various disorders along the x-, y-, and z-axes based on the lattice of model 2. Main chains (z-axis) show a tendency to orient along the fiber axis with some degree of orientation.

Density and Degree of Birefringence

Figures 8 and 9 indicate the draft dependence of the degrees of birefringence Δn and density, respectively. In Δn no change at the transition point is observed. In density a change in slope is observed between the lower and higher draft than the transition point. The degrees of birefringence (Δn) reflect the orientation of phenyl groups in the plane perpendicular to the fiber axis. Other orientations of phenyl groups such as arrangement along the z-axis hardly influence Δn. The first negative peak in $D_2(r)$ increases continuously without any drastic change as draft increases. The reason of no drastic change in draft dependence of Δn is thus explained. For density of polystyrene, the intermolecular phenyl group packing is as important as the intramolecular one. In the range of lower draft than the transition point, the phenyl groups in a chain are inclined to orient in the plane perpendicular to the fiber axis, and packings for the direction of the chain axis become closer but intermolecular orientation scarcely occurs. The density increases as intramolecular packing increases. In the range of higher drafts, both the intramolecular and the intermolecular phenyl groups are packed more closely and the density increases further. Density observations (Fig. 9)

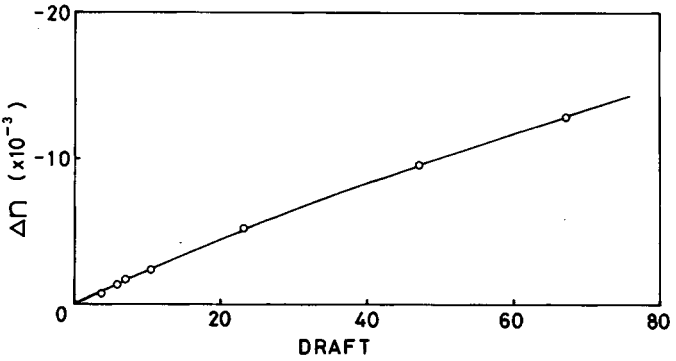

Fig. 8. Dependence of degree of birefringence (Δn) on draft of atactic polystyrene shown in Table I.

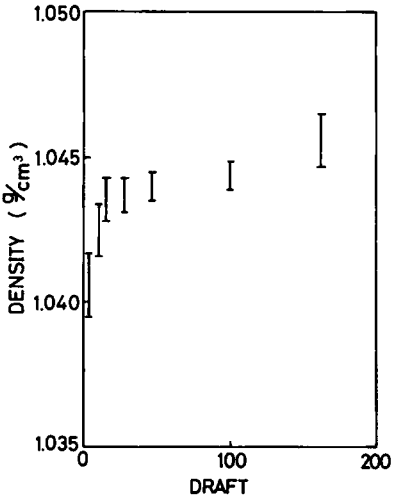

Fig. 9. Dependence of previously measured[8] density of atactic polystyrene monofilaments on draft.

show that intramolecular packing of phenyl groups is more effective when density increases.

Brittle-to-Ductile Transition

It is most probable that brittle fracture results from formation and growth of cracks inside or on the surface of polystyrene monofilaments. In relation to this brittle-to-ductile-transition, the mechanism of formation and growth of cracks is to be investigated more systematically. Tentatively, using our results on amorphous oriented structure of polystyrene monofilaments, this transition is interpreted as follows. In the brittle fracture region, $|\Delta n| \lesssim |-2 \times 10^{-3}|$, intrachain phenyl groups tend to orient perpendicularly to fiber axis or chain axis, but interchain phenyl groups rarely tend to orient, and it is assumed that almost the same packing state is realized as in the completely amorphous state. The existence of empty spaces is supported by lower density and penetration of ethanol into monofilaments. In this region cracks are readily formed and grow as well as in the completely amorphous state and lead to brittle fracture.

In the ductile region $|\Delta n| \gtrsim |-2 \times 10^{-3}|$, interchain phenyl groups tend to orient to the direction of the fiber axis. A likely model for interchain packing is given by model 2 shown in Figure 7. More detailed observation of $D_2(r)$ reveals that the negative peak near $r = 1.6$ Å and the positive peak near $r = 4$ Å increase simultaneously with increase in draft. This simultaneous rise of degree of orientation of phenyl groups in the lateral and longitudinal directions of the fiber axis suggests that main chains are inclined to arrange more and more in parallel with the fiber axis. In these structures, cracks which grow perpendicularly to the fiber axis under external forces are hardly ever formed among these parallel chains. If any were formed, their growth would be stopped by the surrounding oriented chains. Accordingly, suited orientation of main chains parallel to the fiber axis is very important to prevent growth or extension of cracks. Stopping of crack growth results in ductile fracture in atactic polystyrene.

CONCLUSIONS

Atactic polystyrene monofilaments having various degrees of orientation were obtained by the spinning method where molten polystyrene is extruded directly into the surrounding air (+12°C). The brittle-to-ductile transition caused by amorphous orientation was observed in various mechanical properties. The transition point appears in the vicinity of $\Delta n = -2 \times 10^{-3}$ at room temperature of 20°C, stretching rate 100%/min, and relative humidity lower than 65%.

Cylindrically symmetric amorphous orientation was investigated by wide-angle x-ray scattering experiments. The amorphous orientation of these atactic polystyrene monofilaments and its relationship to brittle-to-ductile transition were discussed. The major conclusions of this study may be summarized as follows.

1. In real space the amorphous orientation can be described by the following polar angle α dependence:

$$P_2(\cos \alpha) = \frac{3 \cos^2 \alpha - 1}{2}$$

This also applies to reciprocal space.

2. The deviation from the isotropic distribution function, $D_2(r)$, has two main peaks at lower spacings, in which the negative first peak represents a phenyl group orientation in a plane perpendicular to the fiber axis and the positive second peak represents piling-up of phenyl groups along the direction of the fiber axis. Thie orientational characteristics is interpreted on the basis of the planar zigzag conformation of syndiotactic polystyrene.

3. The negative first peak increases monotonically with increasing draft, which causes a monotonical increase in $|\Delta n|$ in its dependence on draft and no drastic change at the transition point.

4. The behavior of the positive second peaks is different between the brittle and ductile regions. In the brittle region, its position is in the vicinity of $r = 5$ Å, which corresponds to the intramolecular distance between the second-nearest neighbor phenyl groups in a planar zigzag conformation of syndiotactic polystyrene. In the ductile region, it is in the vicinity of $r = 4$ Å. This difference of peak position is due to the existence of interchain phenyl groups at distances $r = 5 \sim 6$ Å in a plane perpendicular to the fiber axis.

5. In the brittle region, $|\Delta n| \lesssim |-2 \times 10^{-3}|$, there are larger empty spaces. Cracks inside or on the surface of the polystyrene monofilaments are formed and are caused to grow by a smaller external force. In the ductile region, $|\Delta n| \gtrsim |-2 \times 10^{-3}|$, the interchain phenyl groups tend to pack at spacings of 5–6 Å in a plane perpendicular to the fiber axis, and chain segments tend to pack parallel to the fiber axis. This parallel packing along the fiber axis suppresses the formation and growth of cracks and leads to ductile fracture.

6. The above-mentioned interpretation of the amorphous orientation of polystyrene is not in conflict with density observation.

The authors are greatly indebted to Professor T. Seto of Tokyo Metropolitan University for valuable discussions and advice about results of x-ray scattering experiments and to Mr. T. Kurita of this laboratory for the spinning of polystyrene. They also wish to thank the members of the Polymer Physics Laboratory in this Research Institute for helpful discussions during the course of this work.

References

1. Y. Tanabe and H. Kanetsuna, *J. Appl. Polym. Sci.*, **22,** 1619 (1978).
2. K. J. Cleereman, H. J. Karam, and J. L. Williams, *Mod. Plast.*, **30,** 119 (1953).
3. M. E. Milberg, *J. Appl. Phys.*, **33,** 1766 (1962).
4. M. E. Milberg and M. C. Daly, *J. Chem. Phys.*, **39,** 2966 (1963).
5. M. E. Milberg, *J. Appl. Phys.*, **34,** 722 (1963).
6. M. E. Milberg, *J. Polym. Sci. A-1,* **1,** 801 (1966).
7. S. M. Wecker, T. Davidson, and J. B. Cohen, *J. Mater. Sci.*, **7,** 1249 (1972).
8. Y. Tanabe and H. Kanetsuna, unpublished work.

Received December 23, 1976
Revised April 14, 1977